A Comprehensive Model for Correlated Drain and Gate Current Fluctuations

W. Goes*, M. Toledano-Luque†, O. Baumgartner*, F. Schanovsky*, B. Kaczer†, and T. Grasser*
*Institute for Microelectronics, TU Wien, Vienna, Austria †imec, Leuven, Belgium

Introduction

Decades ago Andersson *et al.* [1] studied in detail the occurrence of gate current fluctuations in MOS tunnel diodes. As random telegraph noise (RTN) in the drain current has emerged as a serious reliability issue for MOS devices, recent investigations [2, 3] revealed that the fluctuations in the drain and the gate current can be correlated (see Fig. 1). The drain noise has also been investigated in the context of the bias temperature instability (BTI) and is traced back to the capture and emission of substrate charge carriers in the gate oxide. It may be argued that the captured charge locally repels the inversion layer thereby decreasing the direct tunneling current. However, the gate current fluctuations due to this effect can be ruled out due to their small magnitude [4].

Andersson et al. suggested a microscopic picture, in which the capture and emission processes are simply described by a SRH theory. As shown in [5], such a model cannot account for the features usually observed in BTI and noise measurements [5]. However, a multistate model based on nonradiative multiphonon (NMP) processes [6, 7] was proposed that is consistent with all these observations: (*i*) It yields uncorrelated capture (τ_{cap}) and emission (τ_{em}) times. (*ii*) It predicts a strong field dependence of τ_{cap}, ascribed to different curvatures in adiabatic potentials. (*iii*) It can explain the frequency dependence of τ_{cap} by the introduction of an additional metastable state [8]. As an additional benchmark of this model we apply the multistate model to explain correlated drain and gate current fluctuations.

Modeling

The trapping dynamics in the multistate model [5] are illustrated by the state diagram in Fig. 2. In this model the defect features two charge states (positive and neutral) with each having a secondary metastable state besides its equilibrium configuration. The actual hole capture or emission proceed via an NMP transition, whose corresponding rate k can be formulated as an energy integral of the form

$$k = k_0 \int D_{\mathrm{p}}(E) f_{\mathrm{p/n}}(E) \lambda_{\mathrm{p}}(E) f(c_i, c_f, \Delta q_{\mathrm{s}}, \Delta E) \mathrm{d}E. \quad (1)$$

$D_{\mathrm{p}}(E)$ and $\lambda_{\mathrm{p}}(E)$ denote the valence band density of states in the inversion layer and the hole WKB factor, respectively. $f_{\mathrm{p/n}}(E)$ is the occupancy with the corresponding charge carrier type and $f(c_i, c_f, \Delta q_{\mathrm{s}}, \Delta E)$ the semiclassical lineshape function (see Fig. 3). The latter gives the probability for an NMP transition and is associated with the intersection of two adiabatic potential energy surfaces along a reaction path. These potentials are usually described by harmonic oscillators, whose parabolic potentials are defined by their curvatures c_i and c_f, their spatial distance Δq_{s}, and their energy separation ΔE in a configuration coordinate diagram ($\Delta E = E - E_{\mathrm{t}}$ for hole capture and $\Delta E = E_{\mathrm{t}} - E$ for hole emission with E_{t} being the trap level). In this study we employ an analytical form [9] for the high-temperature limit of the lineshape function. It accounts for the quadratic electron-phonon coupling using different curvatures of the two parabolic potentials ($c_i \neq c_j$) and is proven to give an excellent approximation at usual device operation temperatures. Also, all combinations of NMP transition rates for electrons and holes from the substrate and the poly gate have been incorporated into our simulations. Besides those NMP transitions, the state diagram in Fig. 2 also involves pure thermal transitions, which are associated with a structural rearrangement and modeled using Arrhenius-type expressions [5].

The full hole capture process encompasses the transition pathway from the neutral state 1 to the positive state 2 over the metastable state $2'$ while the respective emission process simply proceeds in the reverse direction. Their respective rates are calculated using first passage times. The trap-assisted tunneling (TAT) current responsible for the gate leakage fluctuations is assumed to be caused by the transitions $1'_{\mathrm{s}} \leftrightarrow 1'_{\mathrm{p}}$ over the state 2 as outlined in Fig. 2.

Results

The multistate model was tested for its ability to also correctly predict the gate leakage fluctuations. For this purpose, we evaluated the model against the experimental data for the nanoscaled pFET device investigated in [2]. Fig. 4 demonstrates that the field and temperature dependence observed for the magnitude of the gate fluctuations is well reproduced by the multistate model. Interestingly, the data exhibit no temperature activation, usually reminiscent of some kind of elastic tunneling. The defect in our fits is located close to the substrate interface ($x_{\mathrm{t}} = 4$ Å) so that the hole capture and emission with the substrate occurs on much shorter timescales than the hole emission into the poly gate. As a consequence, the gate leakage is controlled by the NMP transitions rate $2 \rightarrow 1'_{\mathrm{p}}$, whose configuration coordinate diagram is depicted in Fig. 5. Considering all bandstates, the integral (1) has its dominant contributions from the bandstates that intersect the parabola U_2 around its minimum. These transitions feature negligible NMP barriers so that the overall transition k yield no temperature activation. The multistate model also yields a good agreement for the capture and emission times extracted from the noise measurement (see Fig. 6). Both simulations were carried out for the same set of parameters in order to ensure that the model captures both the gate leakage and the trapping phenomenon at the same time.

Conclusion

This study successfully demonstrates that the multistate model not only describes the charge capture and emission as in BTI and RTN but also gives an explanation for the gate fluctuations caused by TAT. As such, the multistate model provides a comprehensive description of oxide defects causing BTI and gate leakage, thereby further corroborating the validity of this model.

Acknowledgements

This work has received funding from the Austrian Science Fund (FWF) project n° 23390-N24 and the European Communitys FP7 n° 261868 (MORDRED).

References

[1] M. Andersson et al., Phys.Rev.B **41**, 9836 (1990).
[2] M. Toledano-Luque et al., Proc.IRPS (2012).
[3] C.-Y. Chen et al., Proc.IRPS (2011).
[4] O. Baumgartner et al., Proc.SISPAD (2008).
[5] T. Grasser et al., Proc.IRPS (2010), pp. 16 –25.
[6] K. Huang et al., Proc.RoyalSoc. of London. Ser. A **204**, 406 (1950).
[7] A. Palma et al., Phys.Rev.B **56**, 9565 (1997).
[8] T. Grasser et al., Proc.IEDM (2012), pp. 19.6.1–19.6.4.
[9] F. Schanovsky et al., Journ. Comp. Electronics **11**, 218 (2012).

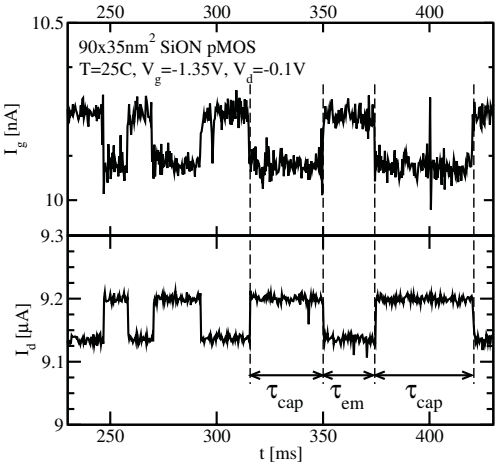

Fig. 1. Simultaneously recorded I_g (upper panel) and I_d traces (lower panel) [2]. Upon the hole capture (after a time period of τ_{cap}), the charged defect reduces I_d to a lower level for electrostatic reasons. At the same time a significant increase in I_g is observed, meaning that an additional conductive path over the defect has been opened. When the hole is emitted after a time period of τ_{em}, I_d returns to its previous level and the conductive path is closed again.

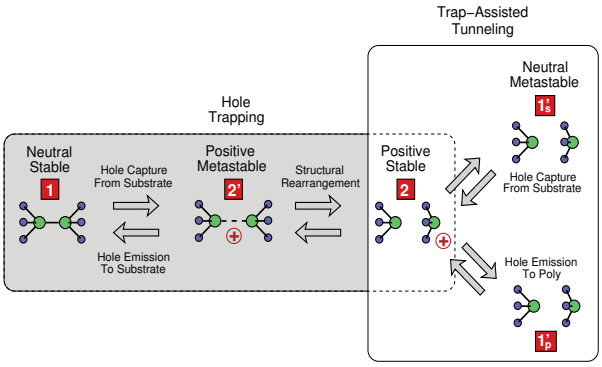

Fig. 2. State diagram of the multistate model. The defect is present in a neutral (1, 1′) and a positive (2, 2′) charge state, where each of them has a second metastable state marked by the prime (1′, 2′). The NMP transitions $1 \leftrightarrow 2'$ and $2 \leftrightarrow 1'$ occur between different charge states while the thermal transitions $2 \leftrightarrow 2'$ connect the positive states 2 and 2′. The subscripts s and p refer to the case where the hole is in the substrate or the poly gate.

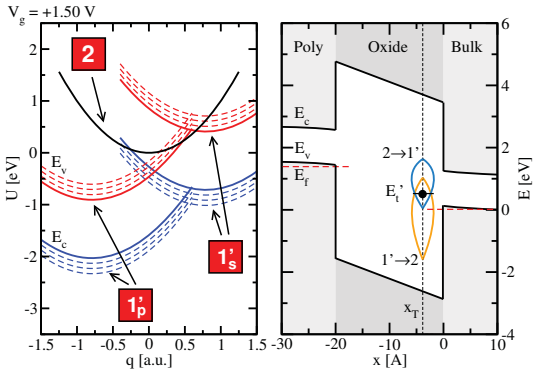

Fig. 3. Left: Adiabatic potential energy surfaces extracted from the fits to the pMOS in [2]. Our simulations consider NMP transitions from all conduction (blue) and valence (red) band states involving charge carriers from the poly gate (left) and the bulk (right). Right: Lineshape functions for the transition $1' \leftrightarrow 2$ plotted into the bandenergy diagram. The width of the lineshape functions corresponds to the probability for the respective NMP transition and can be envisioned as a density of trap levels. There are two different lineshape functions, one for hole capture (orange) and one for hole (turquoise) emission. The thermodynamic trap levels E_t' is located at the point where their respective lineshape functions intersect.

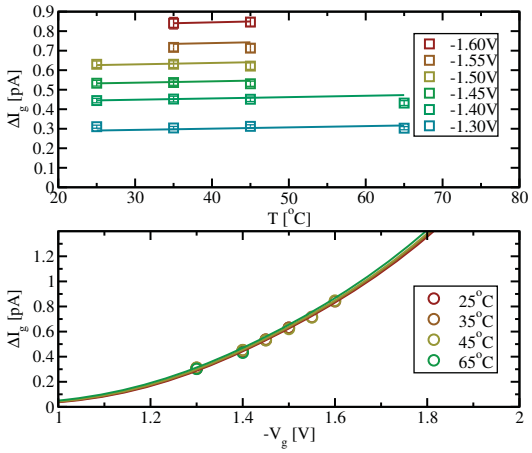

Fig. 4. The step heights of the I_g fluctuations vs. temperature for different gate biases (upper panel). The experimental data (syms) show virtually no temperature dependence — a fact that is usually not associated with a transition over an NMP barrier. Nevertheless, the fit to the experimental data demonstrates that the multistate model is capable of explaining this surprising behavior for reasons given in Fig. 5. The same data are plotted as a function of the gate bias (lower panel).

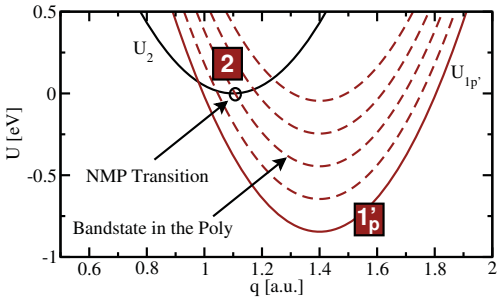

Fig. 5. Schematic configuration coordinate diagram for the transition $2 \rightarrow 1'_p$. The red and the black parabola correspond to the case where the hole is located at the poly or the defect, respectively. When the full width of valence band states (red dashed parabolas) is taken into account, there always exists one red parabola that intersects the black one in its minimum. Then the NMP transition proceeds without a barrier and therefore shows no temperature dependence. Note, however, that for different gate biases different band states become dominant, which affects the WKB factor and gives rise to the observed field dependence in Fig. 4.

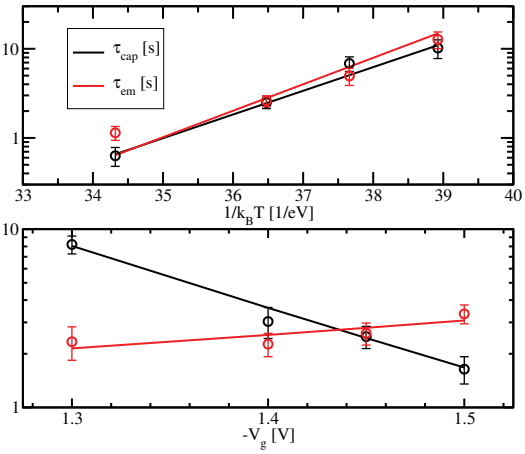

Fig. 6. Comparison of measured (syms) and simulated (lines) for τ_{cap} and τ_{em}. A good agreement with the experimental data is obtained for the temperature (upper panel) and the gate bias (lower panel) dependence.